High precision noble gas measurements of hydrothermal quartz reveal variable loss rate of Xe from the Archean atmosphere

M.W. Broadley [a],[*], D.J. Byrne [a], L. Ardoin [a],[b], M.G. Almayrac [a], D.V. Bekaert [a],[c], B. Marty [a]

[a] Université de Lorraine, CNRS, CRPG, F-54000 Nancy, France
[b] Laboratoire de Glaciologie, Université Libre de Bruxelles, B-1050 Brussels, Belgium
[c] Marine Chemistry and Geochemistry Department, Woods Hole Oceanographic Institution, Woods Hole, MA 02543, USA

A R T I C L E   I N F O

A B S T R A C T

Determining the composition of the Archean atmosphere and oceans is vital to understanding the environmental conditions that existed on the surface of the early Earth. The analysis of atmospheric remnants in fluid inclusions trapped in Archean-aged samples has shown that the Xe isotopic signature of the Archean atmosphere progressively evolved via mass-dependent fractionation, arriving at a modern atmospheric composition around the Archean-Proterozoic transition. The mechanisms driving this evolution are however not well constrained, and it is not yet clear whether the evolution proceeded continuously or via episodic bursts. Providing further constraints on the evolution of Xe in the Archean atmosphere is hampered by the limited amounts of atmospheric gas trapped within fluid inclusions during mineral formation, which impacts the precision at which the Archean atmosphere can be determined. Here, we develop a new crush-and-accumulate extraction technique that enables the heavy noble gases (Ar, Kr and Xe) released from crushing large quantities of hydrothermal quartz to be accumulated and analysed to a higher precision than was previously possible. Using this new technique, we re-evaluate the composition of atmospheric gases trapped within fluid inclusions of 3.3 Ga quartz samples from Barberton, South Africa. We find that the Xe isotopic signature is fractionated by $+10.3 \pm 1.0‰u^{-1}$ (2 SE) relative to modern atmosphere, which is within uncertainty of, but slightly lower than, the previous determination of $12.9 \pm 2.4‰u^{-1}$ for this sample (Avice et al., 2017). We show for the first time that the Kr/Xe ratio measured within Archean quartz samples is enriched in Xe compared to the modern atmosphere, demonstrating that the atmosphere has lost Xe since the Archean. This further reinforces the proposal of atmospheric escape as the primary mechanism for Earth's Xe loss. We further show that the atmospheric Kr/Xe and Xe isotope fractionation recorded in the Barberton quartz at 3.3 Ga is incompatible with a model describing atmospheric loss at a continuous rate under a constant fractionation factor. This gives credence to numerical models of hydrodynamic escape, which suggest that Xe was lost from the Archean atmosphere in episodic bursts rather than at a constant rate. Refining the evolution curve of atmospheric Xe isotopes using the new technique presented here has the potential to shed light on discrete atmospheric events that punctuated the evolution of the Archean Earth and accompanied the evolution of life.

1. Introduction

Volatile elements play a critical role in controlling the evolution of the surface of Earth and the potential for life to develop and be sustained over geological time. However, the history of how Earth acquired its volatile-rich atmosphere and oceans, and how these subsequently evolved over time, remains poorly understood (Marty, 2012). Earth's surface has been shaped by the interplay between processes causing its progressive enrichment in volatiles, such as accretionary addition of chondritic/cometary material (Broadley et al., 2020; Marty et al., 2017; Bekaert et al., 2020a,b) and mantle degassing (Marty et al., 2019), and processes leading to its volatile depletion, such as subduction (Holland and Ballentine, 2006; Bekaert et al., 2021) and atmospheric escape (Pepin and Porcelli, 2002; Zahnle et al., 2019).

The Archean Eon represents a particularly important period in Earth's history, as this is when life first started to develop (Nisbet and Sleep, 2001). Yet, because of the limited surviving geological record from this period, relatively little is known about the con-

* Corresponding author.
E-mail address: michael.broadley@univ-lorraine.fr (M.W. Broadley).

ditions that were present on the surface of the Archean Earth. Despite these limitations, investigations of the Archean rock record have revealed that the Archean atmosphere had significantly different elemental and isotopic compositions than its modern counterpart and underwent a transition towards a modern composition at the Archean-Proterozoic boundary (Farquhar et al., 2000; Lyons et al., 2014; Avice et al., 2017, 2018; Ardoin et al., 2022).

One such volatile element that shows a stark difference in composition between the Archean and modern atmosphere is xenon (Xe) (Pujol et al., 2011; Avice et al., 2017, 2018). Previous analyses of quartz and barite fluid inclusions and atmospheric gases trapped in kerogens have shown that Archean-aged samples present Xe isotopic compositions intermediate between the modern atmospheric value and a theoretical endmember U-Xe; (Pepin, 1991) which is thought to represent the starting composition of the atmosphere (Pujol et al., 2011; Bekaert et al., 2018; Marty et al., 2017; Avice et al., 2017, 2018). More specifically, the Xe isotopic composition of the Archean atmosphere is enriched in light isotopes relative to the modern atmosphere, with the evolution from U-Xe towards the modern composition being driven by mass-dependent isotope fractionation (Avice et al., 2018). The magnitude of fractionation in the modern atmosphere compared to its planetary precursor is $\sim$ 4% per atomic mass unit (u). This significant degree of fractionation is unique to Xe, with other noble gases having present-day isotopic compositions much closer to the composition of atmospheric precursors (Avice et al., 2017, 2018).

The isotopic analysis of Xe in samples with varying age has shown that Xe in the atmosphere evolved throughout the Archean and reached a modern-like composition around 2.4 Ga (Avice et al., 2018), likely during the great oxidation event (Ardoin et al., 2022). The mechanism driving this fractionation is however not known. The Xe-specific aspect of this process rules out thermal-driven escape to space during impacts as a potential cause, as this would preferentially affect the lighter noble gases. One mechanism potentially unique to Xe is irradiation-triggered escape (Hébrard and Marty, 2014; Zahnle et al., 2019): out of all the noble gases, Xe has the lowest first ionisation potential, even lower than hydrogen (Hébrard and Marty, 2014). This suggests that, compared to other elements, Xe can be more easily ionised in the atmosphere, and dragged out to space within a photo-ionised hydrogen wind (Zahnle et al., 2019). This process is however sensitive to many parameters, such as the amount of hydrogen present in the atmosphere, the wavelength and flux of solar Extreme Ultra-Violet photons (EUV) reaching the upper atmosphere, and the strength of Earth's magnetic field (Zahnle et al., 2019). A consequence of this model for Xe escape is that the window of environmental conditions under which it could occur is relatively narrow. In particular, the activity of the young Sun, and its propensity to trigger bursts of EUV irradiation is likely to have been highly variable and discontinuous (Tu et al., 2015). Due to the fact that all these parameters significantly evolved over geological times, Xe's escape would be unlikely to have remained consistent over the entirety of the Archean eon (Zahnle et al., 2019). In this case, a memory of these Xe loss/fractionation events may be present in the geological record, and could be used to determine the underlying mechanisms that controlled episodes of Xe escape and atmospheric evolution. However, constraining the degree of Xe isotope fractionation within Archean samples is not straightforward as the primordial, non-radiogenic isotopes used to constrain the degree of mass fractionation (i.e., ^{124,126,128,130}Xe) are not abundant. This can result in considerable uncertainty on the degree of mass dependent fractionation of Xe trapped in a given sample, hindering accurate determination of how atmospheric Xe evolved through time.

Another feature unique to Xe in the modern atmosphere is its depletion by a factor of 8-20 relative to Kr when compared to chondritic meteorite abundances (Pepin and Porcelli, 2002; Bekaert et al., 2020a,b). Taken together with the unique strong mass fractionation of atmospheric Xe isotope, this "missing xenon" forms the atmospheric Xe paradox (Ozima and Podosek, 2002; Bekaert et al., 2020a). Many hypotheses have been put forward to – at least partially – explain the missing Xe paradox, including loss to space and sequestration into terrestrial reservoirs such as shales (Podosek et al., 1981), ice (Wacker and Anders, 1984), continental crust (Sanloup et al., 2005), and Earth's metallic core (Zhu et al., 2014). However, only the loss of ionised Xe to space has so far been shown to simultaneously account for both the Xe depletion and mass-dependent isotope fractionation (Zahnle et al., 2019). Furthermore, atmospheric escape could also account for a comparable depletion/isotope fractionation of xenon in the Martian atmosphere (Cassata et al., 2022). If loss of ionised Xe to space can account for both the "missing xenon" and the high degree of Xe mass fractionation, then the Archean atmosphere should show a concurrent evolution of both the Xe isotope signature of the atmosphere and the Kr/Xe ratio. However, to date there has been no published data on the Kr/Xe of the Archean atmosphere, so it remains to be seen whether both facets of the Xe paradox can be linked together to depict a more comprehensive picture of the atmosphere's evolution through time.

In this study, we detail a new extraction technique that permits the heavy noble gases (Ar, Kr and Xe) released during crushing of mineral-hosted fluid inclusions to be accumulated and analysed to a previously higher level of precision than has previously been achieved. To test this new extraction method, we have reanalysed previously studied 3.3 Ga quartz samples from Barberton, South Africa (Avice et al., 2017). We outline the advantages of this new technique and present, for the first time, an estimate of the Kr/Xe of the Archean atmosphere to evaluate the link between the "missing xenon" and the evolution of Xe isotope in the Archean atmosphere.

2. Samples and analytical methods

2.1. Extraction procedure

Quartz fragments previously separated from the drill core BMGA3-5 from the Barberton greenstone belt, South Africa (Avice et al., 2017), were cleaned in acetone within an ultrasonic bath for 20 minutes before being dried in an oven set at 100 °C for a minimum of three hours. The quartz grains were then handpicked under a binocular microscope to remove grains that contained visible impurities. Cleaned and separated quartz grains were then loaded in two hand-activated crushers (Avice et al., 2018) and attached to a dedicated extraction line. The crushers were baked at 150 °C for a minimum of 24 hours and pumped for a further 5 days in order to remove adsorbed atmosphere and ensure the blank was low and stable. Crushers were then activated several times to release the gas held within the fluid inclusions. The pressure of the gas released during crushing was monitored using a 1-1000 mbar Baratron pressure gauge. Crushing continued until the pressure of released gas plateaued, thus ensuring efficient extraction of the gas trapped in fluid inclusions. The released gas was then expanded into a 150 cm^3 steel bottle submerged in liquid nitrogen for 10 minutes to concentrate Ar, Kr and Xe, as well other volatile species such as N_2 and CO_2. The efficiency of trapping N_2, Ar, Kr and Xe on the stainless steel walls of the bottle at liquid N_2 temperatures was tested prior to the gas extraction from the samples using atmospheric standards. Trapping efficiencies for N_2, Ar, Kr and Xe were found to be >99%. Once the pressure in the line had returned to background levels, the bottle was sealed and the crushers were removed from the line, cleaned and reloaded with new sample material for additional crushing experiments.

The full extraction process was repeated five times, allowing gas from several discrete extraction steps to be accumulated within the steel bottle. Each crusher would contain between 3 to 4 grams of quartz such that a total of 35.31 grams of quartz was crushed over the 10 separate extractions. A total of 11.53 cm³/STP of gas was released and trapped over the course of the crushing extractions, with the majority of it likely being in the form of water vapour (De Ronde et al., 1997). Since precision on the Xe isotope measurements is limited primarily by sample size, this new crush accumulation technique permits noble gases within quartz-hosted fluid inclusions to be analysed to higher precision than was previously attainable (Avice et al., 2018).

2.2. Analytical procedure

The bottle containing the concentrated heavy noble gases, and residual helium and neon that were not effectively trapped, was detached from the dedicated extraction line and attached to the purification line associated with the ThermoFisher Scientific© Helix MC plus mass spectrometer at CRPG. For each analysis, a 2 cm³ aliquot was extracted from the sample bottle. The gas was purified by being passed through an in-line Ti-sponge getter at 650 °C for 10 minutes to remove any remaining active gas species. The heavy noble gases (Ar, Kr and Xe) were then condensed onto an activated charcoal finger held at 77 K for 10 minutes. Residual He and Ne were typically pumped away. Note however that, for one aliquot (#12), Ne isotopes were also measured. Heavy noble gases were then released from the charcoal finger, and Ar was separated from Kr and Xe by trapping the latters on a quartz finger held at 77 K. The separated Ar was then exposed to a further series of hot (550 °C) and cold Ti-sponge getters (50 °C) prior to being admitted into the mass spectrometer for analysis. Argon isotopes were analysed using peak-jumping mode, with ^{40}Ar measured on the axial faraday collector, and ^{36}Ar and ^{38}Ar isotopes were measured on the axial (AX-CDD) compact discrete dynode electron multiplier.

Due to the high abundance of Ar within the samples, a significant amount of residual Ar gas remained within the quartz tube together with the trapped Kr and Xe. Residual Ar was reduced by repeatedly diluting the quartz tube (20 cm³) to the whole purification line (1,500 cm³), with the quartz tube held at liquid nitrogen temperature, before closing the quartz cold finger and pumping away the residual Ar in the rest of the line. Following their separation from the residual Ar, Kr and Xe were released from the quartz tube and purified using the same procedure as Ar. Due to the difficulty in effectively cryo-separating Kr and Xe, both Kr and Xe were admitted into the mass spectrometer at the same time. Krypton and xenon isotopes were measured using peak-jumping mode over 20 cycles, with Xe isotope being measured first followed by Kr isotopes. For Kr isotopes, only the most abundant isotopes (^{82}Kr, ^{83}Kr, ^{84}Kr and ^{86}Kr) were measured in order to expedite the time taken to complete the analysis, although ^{86}Kr is not presented due to a peak-centring failure. A total of twelve 2 cm³ aliquots of gas were extracted from the bottle and analysed for Xe isotopes, with Kr being analysed on the final 5 extracted aliquots. Given the larger abundance of Ar within a single aliquot and the large difference between the isotopic composition of the samples and the atmosphere, Ar isotopes were only determined on the first aliquot.

The large concentrations of Ar also pose a problem for accurately determining the concentrations of Ar, Kr and Xe, since some of the Ar may remain trapped in the quartz finger together with the Kr and Xe. To overcome this issue, we determined the Ar-Kr-Xe concentrations on a 13th and final aliquot of the bottle using newly installed stainless steel cryogenic trap system designed by Cryoscan SAS. This system allows the effective separation of Ar from Kr and Xe, with <2% of the total Ar being left within the Kr and Xe after separation, and <1% of the Kr being lost to the Ar

fraction. The details of this separation protocol are outlined in the supplementary information.

For the one aliquot in which Ne was measured, Ne was trapped on a liquid He-cooled cryotrap head held at 34 K. Helium remaining in the purification line was then pumped away (with the cryotrap head isolated) before Ne was released from the cryotrap at 90 K. The gas was then purified in the same manner as for Ar, Kr and Xe. Neon isotopes were analysed using multi-collection over 60 cycles. A charcoal cold finger next to the ion source was held at 77 K to minimise the contribution from ^{40}Ar^{++} and CO$_2^{++}$. The high mass resolution of the Helix MC Plus (m/Δm $\approx$ 1800) enables the discrimination of the ^{20}Ne peak from ^{40}Ar^{++} and therefore no correction for ^{40}Ar^{++} interference was necessary. For each analysis, the contribution from CO$_2^{++}$ to the ^{22}Ne peak was monitored and corrected for. The CO$_2^{++}$/CO$_2^+$ ratio was 0.046 and corrections for CO$_2^{++}$ to ^{22}Ne were less than 3% on the ^{20}Ne/^{22}Ne ratio.

Mass discrimination and sensitivity of the mass spectrometer were determined by the daily analysis of standards of an atmospheric isotopic composition. Final propagated uncertainties include the external errors, which corresponds to long-term reproducibility (standard deviation) of the standards. Uncertainties on the mean represent the standard error (STD/$\sqrt{n}$, where n is the number of repeat analyses; n = 5 for Kr and n = 12 for Xe), which is justified by the fact that the same well-mixed gas was analysed each time. Blanks were significantly less than 1% for a single aliquot of gas and therefore no blank corrections were applied.

3. Results

The isotopic composition and abundance of Xe measured in each aliquot (n=12) are presented in Supplementary Tables 1 and 3 respectively. Repeat analysis of the gas extracted from the Barberton sample has enabled the Xe isotopic spectrum of the Archean atmosphere to be determined with high precision (Fig. 1). The average Xe isotopic spectrum of the Barberton sample (reported relative to ^{130}Xe) exhibits excesses in the light isotopes ($^{124-129}$Xe) and deficits in the heavy isotopes ($^{131-136}$Xe) when normalised to modern atmosphere, which is characteristic of the Archean atmosphere (Avice et al., 2017). Fitting an error-weighted correlation through the light isotopes ($^{124-129}$Xe) using Isoplot 4.1 software (Vermeesch, 2018) indicates that Xe from the Archean atmosphere contained within the Barberton quartz is fractionated by 10.3 $\pm$ 1.0 ‰ u^{-1} ($\pm$ 2 SE) relative to the modern atmosphere. This is within uncertainty of, but lower than, the value originally reported for Barberton by Avice et al. (2017) (12.9 $\pm$ 2.4 ‰u^{-1}, $\pm$2SE). It should be noted however that Avice et al. (2017) excluded ^{124}Xe and ^{129}Xe from the linear fit as these isotopes appeared to be in deficit relative to the other light isotopes. If the ^{124}Xe and ^{129}Xe are excluded from the reanalysed Barberton sample then the degree of fractionation is calculated to be slightly higher, at 11.3 $\pm$ 1.3 ‰u^{-1} ($\pm$ 2 SE), which is closer to the value previously determined by Avice et al. (2017). Regardless of whether ^{124}Xe and ^{129}Xe are included in the fit, the reanalysis of Barberton as presented in this study is within 2 SE of the original analysis by Avice et al. (2017) for all light isotope ratios apart from ^{129}Xe/^{130}Xe (Fig. 1).

The Kr isotopic composition of each aliquot (n=5) is presented in supplementary table 2. The average Kr isotopic spectrum of the Barberton sample measured in this study is within error of that previously determined by Avice et al. (2017), which is indistinguishable from modern atmosphere (Fig. 2). This confirms that the process(es) responsible for the fractionation of noble gases between the Archean and the present-day atmosphere appear(s) to be specific to Xe. Importantly, we determined, for the first time,
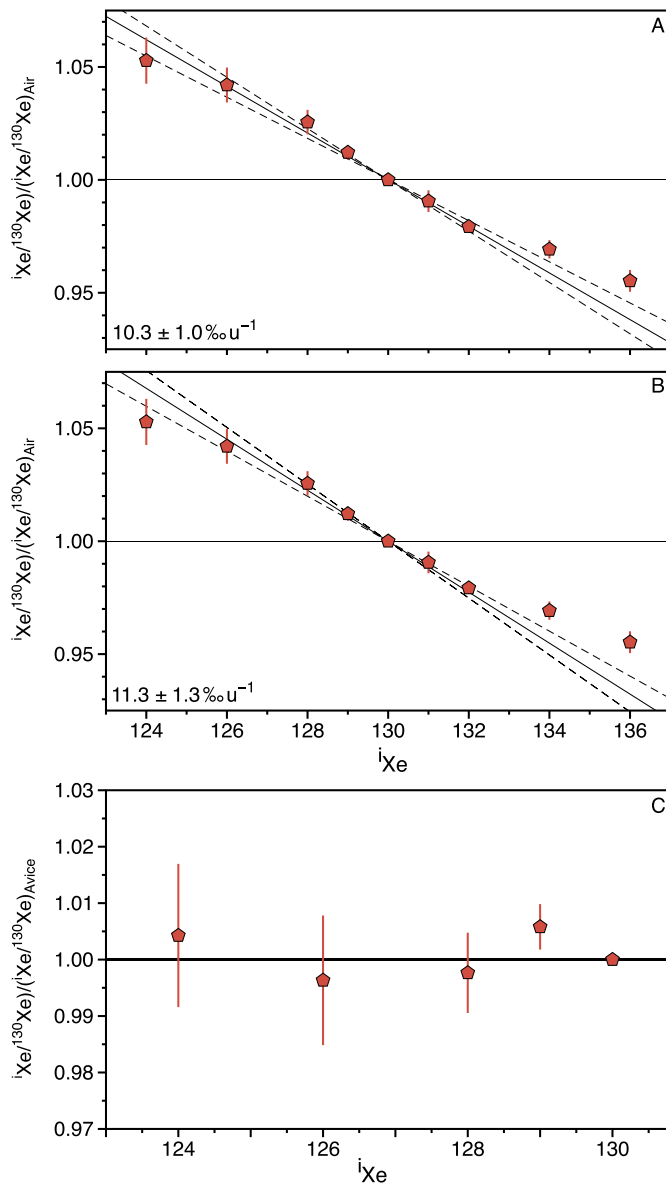
Fig. 1. Xenon isotopic spectra of Barberton quartz hosted fluid inclusions. Data represent the average of 12 aliquots and are normalized to the isotopic composition of atmosphere and ^{130}Xe. The degree of isotopic fractionation is shown by the solid black line and is computed from a line of best fit through using all the light non-fissiogenic Xe isotopes (^{124,126,128,129}Xe) in panel A. In panel B the fit is calculated using ^{126,128,131}Xe in order to compare more effectively with the previous data from Avice et al. (2017). The isotopic fractionation was computed using Isoplot (Vermeesch, 2018) and the error envelope (dashed lines) is 2SE. Uncertainties on the data points represent 2SE (Standard deviation on the mean/$\sqrt{n}$) and are often smaller than symbol size. In panel C the light xenon isotopic spectra of Barberton measured in this study normalised to the previous data from Avice et al. (2017), showing the good agreement with, the exception of ^{129}Xe/^{130}Xe, between the two studies. Uncertainties on the data points are propagated to include the measurement uncertainty from this study and that of Avice et al. (2017).

the abundances of Kr within Barberton fluid inclusions (Supplementary Table 3). We obtain ^{84}Kr/^{130}Xe of 27.2 $\pm$ 1.9 (Supplementary Table 3), which is much lower than the values for both modern atmosphere (184) and modern seawater (103 at 25°C; Ozima and Podosek, 2002).

The one aliquot measured for Ar gave ^{40}Ar/^{36}Ar and ^{38}Ar/^{36}Ar ratios of 5689 $\pm$ 43 and 0.189 $\pm$ 0.002 (1σ), respectively. The ^{40}Ar/^{36}Ar measured within this study for Barberton fluid inclusions is towards the high end of that measured previously during step crushing analysis (2388-8533; Avice et al., 2017), confirming that
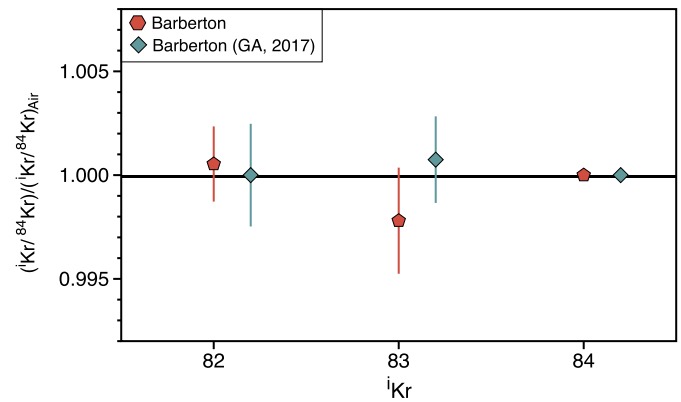

Fig. 2. Krypton isotopic spectra of Barberton quartz hosted fluid inclusions from this study and that of Avice et al. (2017). Data represent the average of 5 aliquots and are normalized to the isotopic composition of atmosphere and ^{84}Kr. Both the data presented in this study and that of Avice et al. (2017) show that the Kr isotopes are within uncertainty of modern atmosphere highlighting that the atmospheric Kr, unlike Xe, has not evolved through time. The light Kr isotopes (^{78,80}Kr) were not measured in this study and due to an analytical issue the ^{86}Kr/^{84}Kr ratio is not presented in this study. Uncertainties on the data points represent 2SE (Standard deviation on the mean/$\sqrt{n}$).
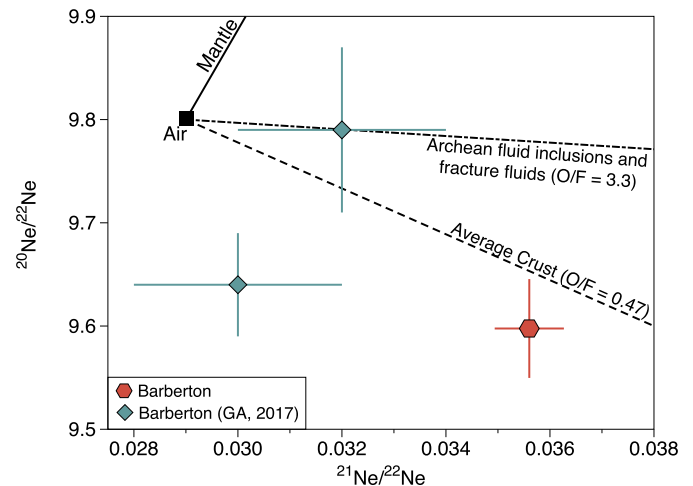

Fig. 3. Three-isotope plot of neon of Barberton quartz hosted fluid inclusions from this study and that of Avice et al. (2017). The mantle-air (Moreira et al., 1998), average crust-air (Kennedy et al., 1990) and Archean fluids-air (Lippmann-Pipke et al., 2011) mixing lines are shown for reference. Errors are 1σ.

the bulk extraction method used in this study extracts gas from the radiogenic fluid inclusions with little modern air contamination. However, one point to note is that the Barberton quartz vein measured here (BMGA3-5) was not measured for Ar in previous studies (Avice et al., 2017).

Meaningful Ne concentrations could not be calculated in this study, as Ne was not effectively trapped on the walls of the steel bottle at liquid nitrogen temperatures. The Ne isotope composition of the sample was however measured from residual Ne within the bottle. The ^{20}Ne/^{22}Ne and ^{21}Ne/^{22}Ne ratios of the Barberton fluids were determined to be 9.60 $\pm$ 0.05 and 0.0356 $\pm$ 0.0006 (1σ), respectively. On a Ne three-isotope plot (Fig. 3), the Barberton fluid inclusions are similar to the modern atmosphere with a slight offset along the average air-crust mixing line (Kennedy et al., 1990). Both ^{21}Ne and ^{22}Ne are primarily produced by (α, n) reactions and thus their production rates are tightly coupled to the preferential siting of U close to their target isotopes of ^{18}O and ^{19}F, respectively (Ballentine and Burnard, 2002). The observed difference between average crustal values, including Barberton, and previously measured Archean fluid inclusions (Lippmann-Pipke et al., 2011) and
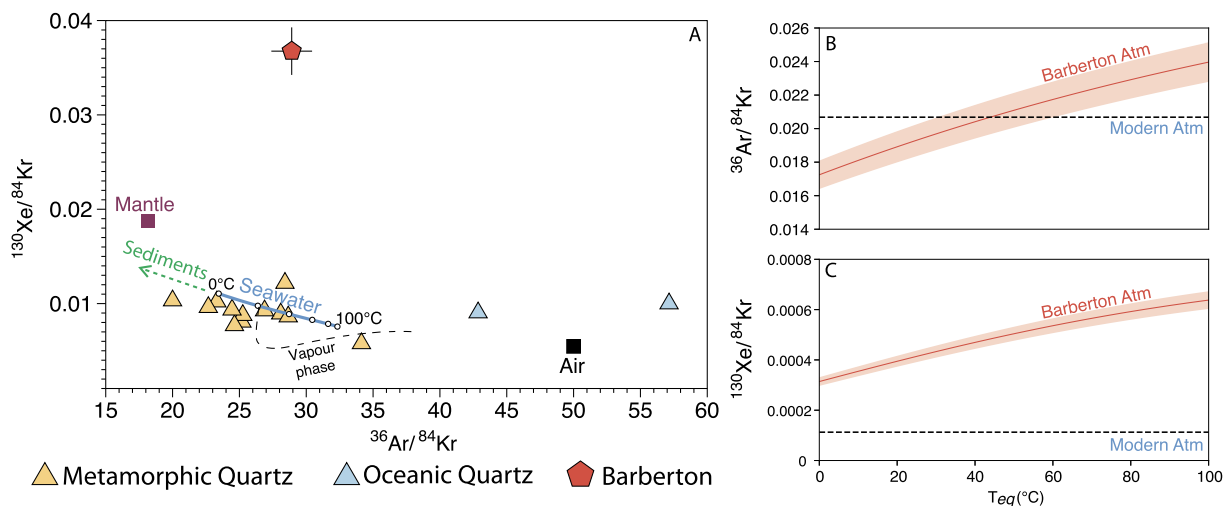
Fig. 4. Heavy noble gas abundance ratios of the Barberton quartz. (A) The sample is plotted relative to air, mantle (Holland and Ballentine, 2006), and crushed fluid inclusions in modern oceanic and metamorphic hydrothermal quartz (Kendrick et al., 2011, 2015). The Barberton sample shows similar ^{36}Ar/^{84}Kr but significantly higher ^{130}Xe/^{84}Kr relative to the modern (<1.5 Ga) metamorphic quartz. This suggests that the Archean atmosphere was more enriched in Xe relative to the modern atmosphere, while Ar and Kr in the atmosphere have remained relatively constant since the Archean. Panels B and C show the expected ^{84}Kr/^{36}Ar and ^{130}Xe/^{36}Ar compositions of the Archean atmosphere over a range of seawater-air equilibration temperatures. The ^{84}Kr/^{36}Ar of Barberton samples (B) show good agreement with seawater values between 30 °C and 60 °C, assuming that the Kr/Ar ratio of the atmosphere hasn't changed since the Archean. The ^{130}Xe/^{36}Ar is elevated above the modern atmosphere over all possible equilibration temperatures once again highlighting that the Archean atmosphere was enriched in Xe relative to the modern atmosphere. The composition of vapours that originated from seawater that equilibrated with the atmosphere at 20 °C, and were generated between 100 °C and the critical point of water (Fernández-Prini et al., 2003), is shown for reference (following the method set out in Byrne et al., 2021).

fracture fluids (Holland et al., 2013) are likely the result of variable O/F ratios, highlighting the fact that crustal Ne production has been heterogeneous since the Archean (Kendrick et al., 2011).

4. Discussion

4.1. Reevaluating the Xe isotopic composition of the Archean atmosphere

The new extraction and concentration analytical procedure developed in this study has many advantages over the previously utilised step crushing technique. Firstly, the same quantity of gas can be analysed each time, thereby increasing the precision on the analysis as it avoids including crushing steps that have low amounts of gas and large uncertainties. Furthermore, as this method accumulates all the gas extracted from crushing, there should be no variation in the composition of the gas between each analysis as may be the case for step crushing. These benefits are exemplified by a more than 50% reduction on the uncertainty for the Xe isotopic fractionation in the Barberton samples compared to the previously published value (Avice et al., 2017). This is despite the fact that the Xe isotopes were only measured 12 times here rather than 27 times using the traditional step crushing method (Avice et al., 2017). In addition, a total mass of 35 g was crushed in this study, compared to ∼54 g for that of Avice et al. (2017). This newly-developed extraction method therefore represents a promising technique for determining the Kr and Xe isotopic composition of gas-poor samples, including paleo-atmospheric proxies such as hydrothermal quartz and mantle minerals. However, it should be noted that using this method results in the loss of information regarding the inherent variations that exist within samples, which only come to light through step crushing. For example, variations in ^{3}He/^{4}He, ^{40}Ar/^{36}Ar and N$_2$/^{36}Ar can arise from variable radiogenic inputs or mixing between different components, allowing for the determination of endmember components (Stuart et al., 1995; Marty et al., 2018; Avice et al., 2017). Future improvements to this method for samples that have not been previously analysed may therefore require He, Ne and Ar isotopes to be measured for each individual crushing step, whilst the Kr and Xe from each crush is

trapped and concentrated in order to obtain the best possible precision on their isotopic analyses.

Despite the overall similarity between the Xe isotope composition of Barberton quartz measured by this study and that of Avice et al. (2017), there are several subtle differences that may have significant consequences for our understanding of atmospheric evolution and mantle degassing processes. Firstly, the most obvious difference between this study and that of Avice et al. (2017) is that the deficit in ^{124}Xe/^{130}Xe relative to the expected degree of fractionation (defined by $^{126, 128, 129, 130}$Xe) found by Avice et al. (2017) was not present in this study (Fig. 1). The reason for the difference between the two studies is not readily apparent, however we note that the measured ^{124}Xe/^{130}Xe are similar between both studies (Fig. 1C).

The ∼20‰ mono-isotopic deficit in ^{124}Xe previously measured in the Barberton quartz was difficult to explain as there are few, if any, processes that can either remove ^{124}Xe from the Archean atmosphere/Barberton sample, or add ^{124}Xe to the modern atmosphere. Avice et al. (2017) considered that the major pathways for ^{124}Xe production (cosmogenic) and decay (thermal neutron capture and subsequent decay to ^{125}Te) would fail to produce the monoisotopic excess and would be too inefficient to result in the ∼20‰ depletion, respectively. The re-evaluation of Xe isotopes in Barberton presented in this study suggests that the apparent ^{124}Xe deficit observed in previous Archean samples (e.g. Avice et al., 2018) may have been simply a statistical artefact arising from the low abundance and thus high uncertainty associated with ^{124}Xe/^{130}Xe measurements. If so, this would resolve one of the most perplexing observations regarding Xe in the ancient atmosphere.

The previous analysis of Barberton quartz also displayed an apparent deficit in ^{129}Xe/^{130}Xe relative to that expected from the degree of mass fractionation constrained by the other non-fissiogenic Xe isotopes (Avice et al., 2017). However, since ^{129}Xe was produced from the decay of extinct ^{129}I, the ^{129}Xe deficit could be readily explained if the Archean atmosphere had lower amounts of radiogenic gases than the modern one. It was therefore assumed that extensive degassing of the mantle, which is enriched in ^{129}Xe (i.e., has a high ^{129}Xe/^{130}Xe) relative to the atmosphere, compen-

sated for this deficit over the ensuing 3.3 Gyr (Avice et al., 2017; Marty et al., 2019). However, in this study we found no such ^{129}Xe deficit in the Barberton fluid inclusions, raising the question as to whether the Archean atmosphere was really deficient in ^{129}Xe and, by extension, whether a period of intense mantle degassing was required to compensate for this apparent deficit (Marty et al., 2019). One possibility that could account for this discrepancy is that the ^{129}Xe content within the fluid inclusions could be variable due to differing inputs from the mantle. However, the involvement of a large mantle ^{129}Xe contribution can for the most part be ruled out given the crustal Ne signature in the sample (Fig. 3). Yet, another potential source of ^{129}Xe in this sample would be from the input of sediments rich in cosmogenic ^{129}I (Holland et al., 2013). Whilst this could potentially supply excess ^{129}Xe to this sample, given that the samples analysed in this study are from the same quartz veins as analysed previously (Avice et al., 2017), such a large variation in sedimentary interaction across repeat aliquots of the same sample is unlikely.

Crucially, potential ^{129}Xe deficits are a secondary observation that can only be calculated relative to the primary observation of mass-dependent fractionation. As this mass-dependent fractionation is usually defined from the less abundant primordial Xe isotopes (and sometimes ^{131}Xe; Avice et al., 2017), variations in how the isotope ratios are calculated, or unconstrained uncertainties on the abundance of these isotopes, could result in significant changes to the calculated mass-dependent fractionation line (Supplementary Figure 2). Further analyses of Archean-aged samples, including those with proposed ^{129}Xe deficits (Avice et al., 2017, 2018; Bekaert et al., 2018), using the extraction technique developed in this study are therefore warranted to firmly establish whether the Archean atmosphere was indeed depleted in ^{129}Xe relative to the modern atmosphere.

4.2. Determining the composition of the ancient atmosphere through the analysis of fluid inclusions

An important corollary of the isotopic evolution of atmospheric Xe by loss to space is that the amount of Xe present in the atmosphere should have also progressively decreased with time. The Archean atmosphere should therefore have a higher Xe/Kr ratio than its modern counterpart. However, discerning the noble gas elemental composition of the ancient atmosphere through the analysis of fluid inclusions is complicated as the abundance of each noble gas in the fluid phase is controlled by its solubility, which in turn depends on both temperature and salinity (Kipfer et al., 2002). Furthermore, other processes that occur within hydrothermal systems, such as boiling (Butterfield et al., 1990; Winckler et al., 2000), water rock interaction, and mantle input (Lupton et al., 1977; Kennedy et al., 1988), can all modify the noble gas elemental composition of the fluids, therefore making it challenging to decipher the atmospheric signature that was originally trapped within the fluid.

Despite the multitude of different inputs and processes that could modify the noble gas elemental signature of hydrothermal fluids, previous work has shown that fluids from hydrothermal vents are dominated by atmospheric noble gases, although with a significant mantle He contribution (Kennedy et al., 1988; Winckler et al., 2000). Furthermore, hydrothermal quartz samples analysed for noble gases have heavy noble gas elemental ratios very close to seawater (Kendrick et al., 2011, 2015), indicating that hydrothermal fluid inclusions may be able to preserve the original noble gas elemental composition that they acquired from equilibration with the atmosphere. For example, metamorphic quartz samples from the Proterozoic Mt Isa ore complex (Australia) have Xe/Kr and Ar/Kr ratios almost identical to the range of values for seawater (Fig. 4). This suggests that, despite the high temperature origin of

the hydrothermal fluids, the increase in salinity, and the potential for interaction within the continental crust (Kendrick et al., 2011), the hydrothermal fluids have retained their original seawater or air-saturated heavy noble gas signature. In addition, hydrothermal quartz samples from the Mathematician Ridge, which are possibly more comparable to the Barberton samples than Mt Isa, given that they also formed in an oceanic setting, likewise maintain seawater like Xe/Kr (Fig. 4; Kendrick et al., 2015). The Mathematician Ridge samples however have Ar/Kr ratios higher (43-57; Fig. 4) than seawater (23-32; Fig. 4), indicating that they may have been affected by some process that has potentially altered the original seawater Ar/Kr ratio (Fig. 4). Care therefore has to be taken when using hydrothermal quartz fluid inclusions to determine the noble gas composition of the paleoatmosphere, as processes such as modern air contamination, fluid-vapour partitioning and sedimentary interaction can all affect the noble gas elemental composition of the trapped fluids. Despite this, many of the modern hydrothermal quartz samples retain modern seawater signatures, demonstrating that important information on the composition of the paleoatmosphere and paleoenvironment can be revealed through the analysis of Archean quartz hosted inclusions (Marty et al., 2018). In particular, the Kr/Xe ratios in quartz inclusions appear to reasonably reflect (paleo)environmental conditions during formation as Fig. 4 demonstrates.

The ^{130}Xe/^{84}Kr ratio of the Barberton fluid inclusions measured in this study is 0.037 ± 0.003 (Supplementary Table 3; Fig. 4), which is significantly higher than modern atmosphere and seawater values. Assuming that the ^{130}Xe/^{84}Kr ratio of Barberton fluid inclusions (Supplementary Table 3) is representative of the surface seawater composition at 3.3 Ga, the ^{130}Xe/^{84}Kr of the ancient atmosphere can be calculated by considering solubility equilibrium between the atmosphere and seawater. As previously mentioned, the solubility of noble gases in seawater is controlled by both salinity and temperature (Smith and Kennedy, 1983). The salinity of the Archean oceans is not well constrained, although from the analysis of halogens and noble gases in Archean-aged hydrothermal quartz samples it has been estimated to be similar to, or slightly lower than, present-day ocean salinity (Marty et al., 2018; Burgess et al., 2020). We therefore assume that Archean seawater had a similar salinity to modern seawater, although since temperature has a much greater influence on noble gas solubility than salinity over the range of likely conditions, changing the seawater salinity would not have a significant effect on our calculations. Taking all this in to consideration, we calculate the ^{130}Xe/^{84}Kr of the Archean atmosphere using the following formulation:

$$\left[\frac{^{130}Xe}{^{84}Kr}\right]_{atm} = \left[\frac{^{130}Xe}{^{84}Kr}\right]_{sw} \times \frac{\gamma_{Xe}K_{Xe}(T)}{\gamma_{Kr}K_{Kr}(T)}$$

Where the subscripts *atm* and *sw* denote the ^{84}Kr/^{130}Xe ratios in the atmosphere and seawater respectively. K_i is the Henry's coefficient for species i and is a function of temperature, and γ_i is the activity coefficient, which accounts for non-ideal behaviour resulting from increased salinity (Fernández-Prini et al., 2003). Taking the minimum and maximum temperature to be the freezing point and boiling point of water respectively, the ^{130}Xe/^{84}Ke of the Archean atmosphere at 3.3 Ga is computed to be between 0.018 and 0.026, significantly higher than the modern-day atmosphere (0.005). Repeating the same calculation using ^{130}Xe/^{36}Ar, instead of ^{84}Kr/^{130}Xe, results in a similar conclusion (Fig. 4C), that the Archean atmosphere was enriched in Xe compared to its modern counterpart.

These results suggest that the Archean atmosphere, trapped in the Barberton quartz inclusions, had higher levels of Xe than at present, and that the progressive isotopic fractionation of Xe in the
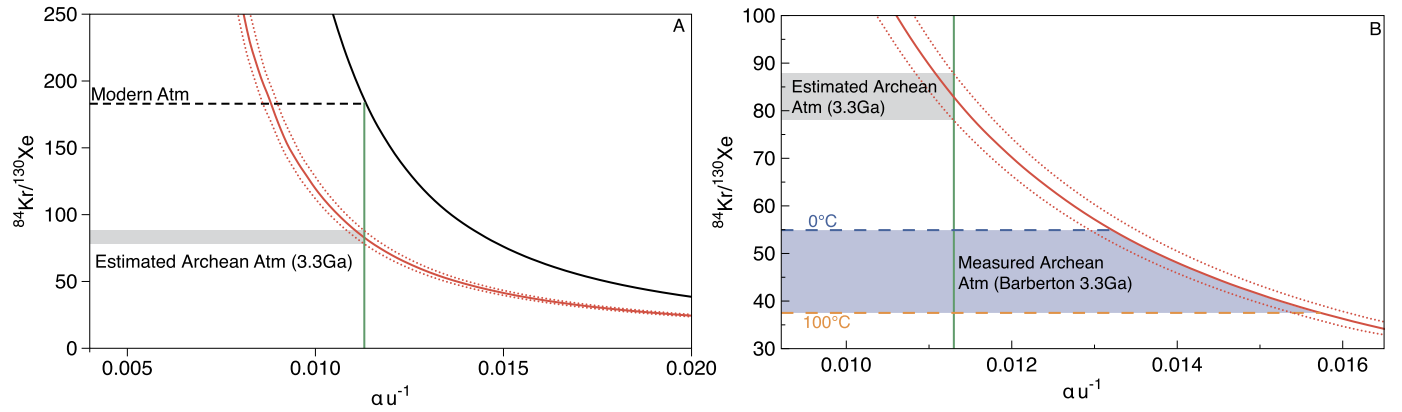
Fig. 5. The $^{84}Kr/^{130}Xe$ of the atmosphere given the degree of isotopic fractionation measured in Archean-aged samples across various fractionation factors (α). Panel A shows that the degree of fractionation from a primordial composition in the modern atmosphere (shown by the solid black line) coupled with an instantaneous fractionation factor of 0.0113 u^{-1} (green line) can successfully account for and the $^{84}Kr/^{130}Xe$ of the modern atmosphere. Assuming that the fractionation factor remained constant through time then the degree of fractionation measured within the Barberton sample (red line) would result in $^{84}Kr/^{130}Xe$ of 82.9 $\pm$ 5 at 3.3 Ga. Panel B represents a zoomed in portion of panel A showing the offset between the estimated $^{84}Kr/^{130}Xe$ at 3.3 Ga when assuming a constant fractionation factor of 0.00113 u^{-1} (grey shaded region) and that measured directly within the Barberton samples (blue shaded region). Dotted lines correspond to the 1σ error on the fractionation measured for Barberton Xe. (For interpretation of the colors in the figure(s), the reader is referred to the web version of this article.)

atmosphere was coupled to the loss of Xe from the atmosphere. Whilst other processes have been proposed to explain the missing Xe in the atmosphere, such as Xe being locked in minerals (Sanloup et al., 2005) or at depth in the core (Zhu et al., 2014), these processes are highly unlikely to (i) produce the isotopic fractionation seen in atmospheric Xe or (ii) quantitatively account for Earth's missing Xe (Bekaert et al., 2020a,b). Here, we find that the $^{130}Xe/^{84}Kr$ ratio of the atmosphere 3.3 Ga was intermediate between the original composition (assumed to be chondritic-like; Holland et al., 2009; Broadley et al., 2020; Bekaert et al., 2020a,b) and the modern atmosphere. This finding would therefore appear to refute the idea that the missing Xe may be stored in the Earth's metallic core or the continental as the formation of these reservoirs is likely to have finished prior to 3.3 Ga (Kleine et al., 2004; Pujol et al., 2013). We therefore conclude that both the isotopic fractionation and loss of Xe from the atmosphere are best explained via escape to space of ionised Xe (Pujol et al., 2011; Hébrard and Marty, 2014; Avice et al., 2018; Zahnle et al., 2019).

4.3. Atmospheric Xenon evolution in the Archean

In the following discussion, we discuss Kr/Xe instead of Xe/Kr in order to facilitate easier comparison between different endmembers. Lower atmospheric Kr/Xe ratios in the Archean coupled with the progressive evolution of Xe isotopes (Avice et al., 2018) suggest that atmospheric Xe was lost to space in Earth's early history. During their escape to space, Xe isotopes would have been fractionated in accordance with their respective masses. Assuming that the isotopic fractionation of Xe was controlled by Rayleigh-type distillation, as originally proposed by Pujol et al. (2011), then the degree of Xe isotopic fractionation at a given time will be directly related to the amount of Xe that has been lost from the atmosphere. Avice et al. (2018) showed that the isotopic composition of Xe in the modern atmosphere, starting from an assumed chondritic starting composition and coupled with a 23-fold abundance depletion (Pepin, 1991), is compatible with a Rayleigh distillation-type process. Taking the degree of Xe fractionation measured within an Archean sample relative to its starting composition (δXe_{UXe}), we can calculate the Kr/Xe of the Archean atmosphere assuming a given range of fractionation factors (α). Assuming that Kr has been conservative in the atmosphere, then the Kr/Xe of the Archean atmosphere at the time of sample formation (Kr/Xe$_{Atm}$) can be expressed as:

$$\left[\frac{Kr}{Xe}\right]_{Atm} = \left[\frac{Kr}{Xe}\right]_{chon} \times \frac{1}{f}$$

where Kr/Xe$_{chon}$ is the composition of the initial atmosphere, assumed to be chondritic ($^{84}Kr/^{130}Xe = 5.0 \pm 0.3$; Busemann et al., 2000) and f is the fraction of Xe remaining in the atmosphere (i.e., $f = \frac{Xe_{Atm}}{Xe_{Chon}}$). The fraction of Xe remaining in the atmosphere can then be calculated following the approach of Avice et al. (2018), where:

$$f = \left(1 - \frac{\delta Xe_{UXe}}{1000}\right)^{\frac{1}{\alpha}}$$

Fig. 5 shows that an instantaneous isotopic fractionation factor (α) of 0.0113 u^{-1} can simultaneously account for the degree of Xe isotope fractionation from U-Xe and the $^{84}Kr/^{130}Xe$ of the modern atmosphere. Assuming that α is constant through time, then, given the degree of fractionation found within the Barberton samples, we predict the atmosphere at 3.3 Ga to have had $^{84}Kr/^{130}Xe$ of 82.9 $\pm$ 5 (1σ; Fig. 5). The $^{84}Kr/^{130}Xe$ measured within the Barberton samples however suggests that the $^{84}Kr/^{130}Xe$ of the atmosphere 3.3 Ga was between 38 and 55, depending on the temperature at which the atmosphere was equilibrated with seawater. The measured values $^{84}Kr/^{130}Xe$ are therefore lower than what is predicted assuming a constant fractionation factor and a constant rate of loss through time.

The most recent and comprehensive model for how Xe was uniquely lost to space suggests that, because of its ionisation potential being lower than other noble gases, Xe can be easily photo-ionised and then transported as ions within a photo-ionised hydrogen wind, that may have travelled along polar magnetic field lines (Zahnle et al., 2019). Crucially, this model predicts that Xe was lost from the atmosphere in episodic bursts associated with changes in the Earth's magnetic field or increased solar EUV activity, rather than through a constant flux to space (Zahnle et al., 2019). The mismatch between the modelled $^{130}Xe/^{84}Kr/$ when assuming a constant fractionation factor (α) and the ancient atmospheric $^{84}Kr/^{130}Xe$ ratio calculated here from the Barberton data suggests that Xe loss from the atmosphere was variable over time and potentially occurred in isolated bursts, when the right conditions for Xe escape to space prevailed. Variable atmospheric Xe loss, or different loss events, would be associated with different degrees of isotope fractionation dependent on the different factors controlling the escape.
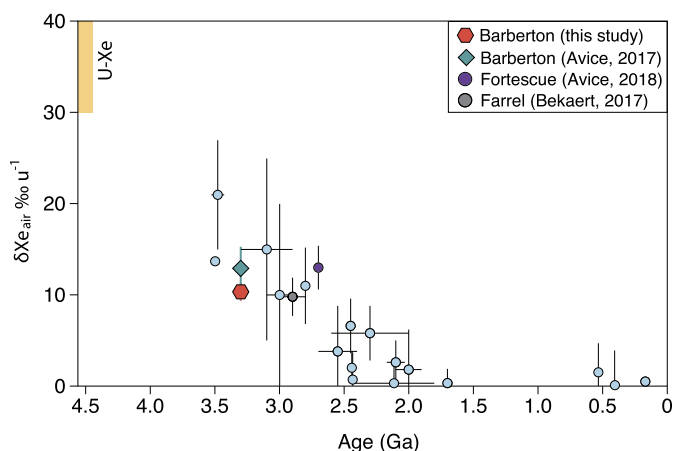
Fig. 6. Evolution of atmospheric Xe isotopes revealed by the analysis of samples of varying ages (Ardoin et al. (2022) and reference therein). Xenon in the atmosphere evolves from a starting atmospheric composition (U-Xe; Pepin (1991)) before reaching a modern composition around 2.5 Ga. The re-evaluated Barberton sample is lower than the previous measurement (Avice et al., 2017) but still fits well with the Xe evolution curve. Xenon isotope compositions are expressed in per mil variation per atomic mass unit ($‰ u^{-1}$) relative to the modern atmosphere. Errors are shown to 2σ.

4.4. Redefining the atmospheric Xe evolution curve

Our current understanding of how atmospheric Xe evolved in the Archean atmosphere is based on a very limited amount of data such that the atmospheric Xe evolution curve (Fig. 6) is at a very low resolution. For instance, the newly redefined Xe signature of the 3.3 billion year-old Barberton samples now appears more fractionated (from a U-Xe starting composition) than that previously measured in quartz samples from the Fortescue Group (Australia), which formed over 500 million years after Barberton (Avice et al., 2018), although at 2σ both samples are within uncertainty (Fig. 6). The difference between the two samples could be a consequence of the differences in the employed extraction techniques, such that future analyses of Fortescue using the new extraction technique presented in this study may produce a lower degree of Xe isotope fractionation, as is the case for Barberton, potentially bringing it back in line with the purported atmospheric evolution curve (Fig. 6). Nevertheless, the previously suggested roughly 500 million-year lull in atmospheric Xe fractionation (Avice et al., 2018; Almayrac et al., 2021) may still stand as the newly revised Barberton Xe fractionation ($10.3 \pm 1.0‰ u^{-1}$) is similar to that found in organic matter extracted from the 3.0 billion year old Farrel Quartzite, Australia ($9.8 \pm 2.1\% u^{-1}$; Bekaert et al., 2018). Determining whether Xe loss to space was quasi-constant or indeed progressed in a discontinuous fashion related to changes in the composition of the atmosphere, the Earth's magnetic field, and/or solar activity, will require future analyses of Xe isotopes in Archean samples to reach a greater precision than currently achieved, potentially using the extraction technique developed as part of this study.

5. Conclusions

We present noble gas data from fluid inclusions in hydrothermal quartz from Barberton, South Africa, collected using a new crush and concentrate technique which has permitted the noble gas composition of the Archean atmosphere to be determined to higher levels of precision than previously attained. The isotopic composition of Xe in the Barberton samples is similar to previously reported results, with values intermediate between the modern atmosphere and the primordial U-Xe component, confirming that the isotopic composition of Xe evolved through time. Unlike previous

studies of Archean quartz, we find no deficit in ^{124}Xe and ^{129}Xe, indicating that a period of intense mantle degassing at the end of the Archean eon may not be required to compensate for the deficit in ^{129}Xe. Krypton isotope ratios, unlike Xe, are identical to modern atmosphere, confirming that mass dependent isotope fractionation in the Archean was a process unique to Xe. Furthermore, we suggest that the Barberton quartz has faithfully recorded the Kr/Xe ratio of the Archean seawater, and by connection the Archean atmosphere. The Kr/Xe of the Archean atmosphere appears to be lower than its modern counterpart. The identification of fractionated Xe isotopes coupled with low Kr/Xe in the Archean atmosphere provides strong evidence that Xe loss to space is the primary reason for the extreme depletion (relative to Ar and Kr) and the highly fractionated isotopic signature of atmospheric Xe compared to known cosmochemical precursors.

Finally, comparing the Kr/Xe measured in the Barberton samples with modelled Kr/Xe ratios calculated assuming a constant instantaneous fractionation factor during Xe escape to space reveals that the Kr/Xe ratio measured in the Barberton sample is lower than the range of values predicted at 3.3 Ga. This suggests that Xe was likely lost from the atmosphere in episodic bursts or at variable rates throughout the Archean. These findings are in line with numerical models predicting that ionised Xe was lost from the atmosphere during periods of greater solar activity or changes in the Earth's magnetic field. Future studies using the new crush-and-concentrate technique outlined in this study may be able to offer further insights into the nature and timing of these Xe loss events, with important implications for our understanding of atmospheric evolution and mantle degassing processes.

CRediT authorship contribution statement

M.W. Broadley: Conceptualization, Formal analysis, Investigation, Methodology, Writing – original draft. **D.J. Byrne:** Formal analysis, Writing – review & editing. **L. Ardoin:** Investigation, Methodology, Writing – review & editing. **M.G. Almayrac:** Formal analysis, Writing – review & editing. **D.V. Bekaert:** Formal analysis, Writing – review & editing. **B. Marty:** Funding acquisition, Supervision, Writing – review & editing.

Declaration of competing interest

The authors declare that they have no known competing financial interests or personal relationships that could have appeared to influence the work reported in this paper.

Acknowledgements

Appendix A. Supplementary material

Supplementary material related to this article can be found online at https://doi.org/10.1016/j.epsl.2022.117577.

References

Almayrac, M.G., Broadley, M.W., Bekaert, D.V., Hofmann, A., Marty, B., 2021. Possible discontinuous evolution of atmospheric xenon suggested by Archean barites. Chem. Geol. 120405.

Ardoin, L., Broadley, M.W., Almayrac, M., Avice, G., Byrne, D.J., Tarantola, A., Leplan, A., Saito, T., Komiya, T., Shibuya, T., Marty, B., 2022. The end of the isotopic evolution of atmospheric xenon. Geochem. Perspect. Lett. 20, 43–47.

Avice, G., Marty, B., Burgess, R., 2017. The origin and degassing history of the Earth's atmosphere revealed by Archean xenon. Nat. Commun. 8 (1), 1–9.

Avice, G., Marty, B., Burgess, R., Hofmann, A., Philippot, P., Zahnle, K., Zakharov, D., 2018. Evolution of atmospheric xenon and other noble gases inferred from Archean to Paleoproterozoic rocks. Geochim. Cosmochim. Acta 232, 82–100.

Ballentine, C.J., Burnard, P.G., 2002. Production, release and transport of noble gases in the continental crust. Rev. Mineral. Geochem. 47 (1), 481–538.

Broadley, M.W., Barry, P.H., Bekaert, D.V., Byrne, D.J., Caracausi, A., Ballentine, C.J., Marty, B., 2020. Identification of chondritic krypton and xenon in Yellowstone gases and the timing of terrestrial volatile accretion. Proc. Natl. Acad. Sci. 117 (25), 13997–14004.

Bekaert, D.V., Broadley, M.W., Marty, B., 2020a. The origin and fate of volatile elements on Earth revisited in light of noble gas data obtained from comet 67P/Churyumov-Gerasimenko. Sci. Rep. 10 (1), 1–18.

Bekaert, D.V., Broadley, M.W., Delarue, F., Avice, G., Robert, F., Marty, B., 2018. Archean kerogen as a new tracer of atmospheric evolution: implications for dating the widespread nature of early life. Sci. Adv. 4 (2), eaar2091.

Bekaert, D.V., Broadley, M.W., Delarue, F., Druzhinina, Z., Paris, G., Robert, F., Sugitani, K., Marty, B., 2020b. Xenon isotopes in Archean and Proterozoic insoluble organic matter: a robust indicator of syngenecity? Precambrian Res. 336, 105505.

Bekaert, D.V., Turner, S.J., Broadley, M.W., Barnes, J.D., Halldórsson, S.A., Labidi, J., Wade, J., Walowski, K.J., Barry, P.H., 2021. Subduction-driven volatile recycling: a global mass balance. Annu. Rev. Earth Planet. Sci. 49.

Burgess, R., Goldsmith, S.L., Sumino, H., Gilmour, J.D., Marty, B., Pujol, M., Konhauser, K.O., 2020. Archean to Paleoproterozoic seawater halogen ratios recorded by fluid inclusions in chert and hydrothermal quartz. Am. Mineral. 105 (9), 1317–1325.

Byrne, D.J., Broadley, M.W., Halldórsson, S.A., Ranta, E., Ricci, A., Tyne, R.L., Stefánsson, A., Ballentine, C.J., Barry, P.H., 2021. The use of noble gas isotopes to trace subsurface boiling temperatures in Icelandic geothermal systems. Earth Planet. Sci. Lett. 560, 116805.

Butterfield, D.A., Massoth, G.J., McDuff, R.E., Lupton, J.E., Lilley, M.D., 1990. Geochemistry of hydrothermal fluids from axial seamount hydrothermal emissions study vent field, Juan de Fuca Ridge: subseafloor boiling and subsequent fluid-rock interaction. J. Geophys. Res., Solid Earth 95 (B8), 12895–12921.

Cassata, W.S., Zahnle, K.J., Samperton, K.M., Stephenson, P.C., Wimpenny, J., 2022. Xenon isotope constraints on ancient Martian atmospheric escape. Earth Planet. Sci. Lett. 580, 117349.

De Ronde, C.E., Channer, D.M.D., Faure, K., Bray, C.J., Spooner, E.T., 1997. Fluid chemistry of Archean seafloor hydrothermal vents: implications for the composition of circa 3.2 Ga seawater. Geochim. Cosmochim. Acta 61 (19), 4025–4042.

Farquhar, J., Bao, H., Thiemens, M., 2000. Atmospheric influence of Earth's earliest sulfur cycle. Science 289 (5480), 756–758.

Fernández-Prini, R., Alvarez, J.L., Harvey, A.H., 2003. Henry's constants and vapor–liquid distribution constants for gaseous solutes in H_2O and D_2O at high temperatures. J. Phys. Chem. Ref. Data 32 (2), 903–916.

Hébrard, E., Marty, B., 2014. Coupled noble gas–hydrocarbon evolution of the early Earth atmosphere upon solar UV irradiation. Earth Planet. Sci. Lett. 385, 40–48.

Holland, G., Ballentine, C.J., 2006. Seawater subduction controls the heavy noble gas composition of the mantle. Nature 441 (7090), 186–191.

Holland, G., Cassidy, M., Ballentine, C.J., 2009. Meteorite Kr in Earth's mantle suggests a late accretionary source for the atmosphere. Science 326 (5959), 1522–1525.

Holland, G., Lollar, B.S., Li, L., Lacrampe-Couloume, G., Slater, G.F., Ballentine, C.J., 2013. Deep fracture fluids isolated in the crust since the Precambrian era. Nature 497 (7449), 357–360.

Kendrick, M.A., Honda, M., Oliver, N.H.S., Phillips, D., 2011. The noble gas systematics of late-orogenic H_2O–CO_2 fluids, Mt Isa Australia. Geochim. Cosmochim. Acta 75 (6), 1428–1450.

Kendrick, M.A., Honda, M., Vanko, D.A., 2015. Halogens and noble gases in Mathematician Ridge meta-gabbros, NE Pacific: implications for oceanic hydrothermal root zones and global volatile cycles. Contrib. Mineral. Petrol. 170 (5), 1–20.

Kennedy, B.M., Hiyagon, H., Reynolds, J.H., 1990. Crustal neon: a striking uniformity. Earth Planet. Sci. Lett. 98 (3–4), 277–286.

Kennedy, B.M., Reynolds, J.H., Smith, S.P., 1988. Noble gas geochemistry in thermal springs. Geochim. Cosmochim. Acta 52 (7), 1919–1928.

Kipfer, R., Aeschbach-Hertig, W., Peeters, F., Stute, M., 2002. Noble gases in lakes and ground waters. Rev. Mineral. Geochem. 47 (1), 615–700.

Kleine, T., Mezger, K., Palme, H., Münker, C., 2004. The W isotope evolution of the bulk silicate Earth: constraints on the timing and mechanisms of core formation and accretion. Earth Planet. Sci. Lett. 228 (1–2), 109–123.

Lippmann-Pipke, J., Lollar, B.S., Niedermann, S., Stroncik, N.A., Naumann, R., van Heerden, E., Onstott, T.C., 2011. Neon identifies two billion year old fluid component in Kaapvaal Craton. Chem. Geol. 283 (3–4), 287–296.

Lupton, J.E., Weiss, R.F., Craig, H., 1977. Mantle helium in hydrothermal plumes in the Galapagos Rift. Nature 267 (5612), 603–604.

Lyons, T.W., Reinhard, C.T., Planavsky, N.J., 2014. The rise of oxygen in Earth's early ocean and atmosphere. Nature 506 (7488), 307–315.

Marty, B., 2012. The origins and concentrations of water, carbon, nitrogen and noble gases on Earth. Earth Planet. Sci. Lett. 313, 56–66.

Marty, B., Altwegg, K., Balsiger, H., Bar-Nun, A., Bekaert, D.V., Berthelier, J.J., Bieler, A., Briois, C., Calmonte, U., Combi, M., De Keyser, J., 2017. Xenon isotopes in 67P/Churyumov-Gerasimenko show that comets contributed to Earth's atmosphere. Science 356 (6342), 1069–1072.

Marty, B., Avice, G., Bekaert, D.V., Broadley, M.W., 2018. Salinity of the Archaean oceans from analysis of fluid inclusions in quartz. C. R. Géosci. 350 (4), 154–163.

Marty, B., Bekaert, D.V., Broadley, M.W., Jaupart, C., 2019. Geochemical evidence for high volatile fluxes from the mantle at the end of the Archaean. Nature 575 (7783), 485–488.

Moreira, M., Kunz, J., Allegre, C., 1998. Rare gas systematics in popping rock: isotopic and elemental compositions in the upper mantle. Science 279 (5354), 1178–1181.

Nisbet, E.G., Sleep, N.H., 2001. The habitat and nature of early life. Nature 409 (6823), 1083–1091.

Ozima, M., Podosek, F.A., 2002. Noble Gas Geochemistry. Cambridge University Press.

Pepin, R.O., 1991. On the origin and early evolution of terrestrial planet atmospheres and meteoritic volatiles. Icarus 92 (1), 2–79.

Pepin, R.O., Porcelli, D., 2002. Origin of noble gases in the terrestrial planets. Rev. Mineral. Geochem. 47 (1), 191–246.

Podosek, F.A., Bernatowicz, T.J., Kramer, F.E., 1981. Adsorption of xenon and krypton on shales. Geochim. Cosmochim. Acta 45 (12), 2401–2415.

Pujol, M., Marty, B., Burgess, R., 2011. Chondritic-like xenon trapped in Archean rocks: a possible signature of the ancient atmosphere. Earth Planet. Sci. Lett. 308 (3–4), 298–306.

Pujol, M., Marty, B., Burgess, R., Turner, G., Philippot, P., 2013. Argon isotopic composition of Archaean atmosphere probes early Earth geodynamics. Nature 498 (7452), 87–90.

Sanloup, C., Schmidt, B.C., Perez, E.M.C., Jambon, A., Gregoryanz, E., Mezouar, M., 2005. Retention of xenon in quartz and Earth's missing xenon. Science 310 (5751), 1174–1177.

Smith, S.P., Kennedy, B.M., 1983. The solubility of noble gases in water and in NaCl brine. Geochim. Cosmochim. Acta 47 (3), 503–515.

Stuart, F.M., Burnard, P.G., Taylor, R.E.A., Turner, G., 1995. Resolving mantle and crustal contributions to ancient hydrothermal fluids: He-Ar isotopes in fluid inclusions from Dae Hwa W-Mo mineralisation, South Korea. Geochim. Cosmochim. Acta 59 (22), 4663–4673.

Tu, L., Johnstone, C.P., Güdel, M., Lammer, H., 2015. The extreme ultraviolet and X-ray sun in time: high-energy evolutionary tracks of a solar-like star. Astron. Astrophys. 577, L3.

Vermeesch, P., 2018. IsoplotR: a free and open toolbox for geochronology. Geosci. Front. 9 (5), 1479–1493.

Wacker, J.F., Anders, E., 1984. Trapping of xenon in ice: implications for the origin of the Earth's noble gases. Geochim. Cosmochim. Acta 48 (11), 2373–2380.

Winckler, G., Kipfer, R., Aeschbach–Hertig, W., Botz, R., Schmidt, M., Schuler, S., Bayer, R., 2000. Sub sea floor boiling of Red Sea Brines: new indication from noble gas data. Geochim. Cosmochim. Acta 64 (9), 1567–1575.

Zahnle, K.J., Gacesa, M., Catling, D.C., 2019. Strange messenger: a new history of hydrogen on Earth, as told by Xenon. Geochim. Cosmochim. Acta 244, 56–85.

Zhu, L., Liu, H., Pickard, C.J., Zou, G., Ma, Y., 2014. Reactions of xenon with iron and nickel are predicted in the Earth's inner core. Nat. Chem. 6 (7), 644.